



Effect and Mechanism Study of Sodium Houttuynonate on Ventilator-Induced Lung Injury by Inhibiting ROS and Inflammation

Yi Liu, Gang Tang, and Jinyu Li

Department of Anesthesiology, The Affiliated Huaian No.1 People's Hospital of Nanjing Medical University, Nanjing, Jiangsu, China.

Purpose: Ventilator-induced lung injury (VILI) is a serious complication of mechanical ventilation (MV) that increases morbidity and mortality of patients receiving ventilator treatment. This study aimed to reveal the molecular mechanism of sodium houttuynonate (SH) on VILI.

Materials and Methods: The male mice VILI model was established by high tidal volume ventilation. The cell model was established by performing cell stretch (CS) experiments on murine respiratory epithelial cells MLE-15. In addition, the JNK activator Anisomycin and JNK inhibitor SP600125 were used on VILI mice and CS-treated cells.

Results: VILI modeling damaged the structural integrity, increased apoptosis and wet-to-dry (W/D) ratio, enhanced the levels of inflammatory factors, reactive oxygen species (ROS) and malonaldehyde (MDA), and activated JNK pathway in lung tissues. SH gavage alleviated lung injury, decreased apoptosis and W/D ratio, and reduced levels of inflammatory factors, ROS and MDA, and p-JNK/JNK expression of lung tissues in VILI mice. However, activation of JNK wiped the protective effect of SH on VILI. Contrary results were found in experiments with JNK inhibitor SP600125.

Conclusion: SH relieved VILI by inhibiting the ROS-mediated JNK pathway.

Key Words: Sodium houttuynonate, ventilator-induced lung injury, ROS, inflammation, JNK pathway

INTRODUCTION

Mechanical ventilation (MV) is an important tool for treating patients suffering from acute respiratory distress (ARDS). However, MV can cause ventilator-induced lung injury (VILI), which worsens the condition and increases the likelihood of mortality of patients receiving ventilator therapy.¹ The mechanisms of VILI, including volutrauma, biotrauma, barotrauma, and atelectrauma,² result in the accumulation of inflammatory

cells and the excessive production of inflammatory cytokines, which increase vascular permeability and aggravate pulmonary oedema.³ Currently, the countermeasures to reduce VILI mainly consist of low-tide MV, positive end-expiratory pressure, recruitment maneuvers, and prone position ventilation.^{4,5} Although many studies have focused on the pathogenesis of VILI, the effects of current treatment protocols remain limited. Therefore, investigating more effective therapeutics would be beneficial for developing treatments for VILI.

Sodium houttuynonate (SH) is a compound synthesized by combining sodium bisulfite with houttuynia, the main active extract of *Houttuynia cordata*.⁶ SH inhibits the inflammatory response of mastitis.⁷ A study by Tang, et al.⁸ has shown that SH plays a role in neuroprotection in rats with traumatic spinal cord injury by reducing the neuronal apoptosis. SH protected the lung tissue in chronic obstructive pulmonary disease (COPD) inflammatory rat models by attenuating pulmonary inflammation.⁹ However, the effect of SH on VILI has been poorly studied. Therefore, further studies are needed to further investigate the mechanisms of SH in VILI.

Received: December 8, 2020 **Revised:** February 18, 2021

Accepted: March 16, 2021

Corresponding author: Jinyu Li, BD, Department of Anesthesiology, The Affiliated Huaian No.1 People's Hospital of Nanjing Medical University, Nanjing, Jiangsu 223300, China.

Tel: 86-0517-5914429, Fax: 86-0517-5914429, E-mail: jinyuli3568@163.com

•The authors have no potential conflicts of interest to disclose.

© Copyright: Yonsei University College of Medicine 2021

This is an Open Access article distributed under the terms of the Creative Commons Attribution Non-Commercial License (<https://creativecommons.org/licenses/by-nc/4.0>) which permits unrestricted non-commercial use, distribution, and reproduction in any medium, provided the original work is properly cited.

Dexamethasone induces osteoblasts apoptosis by activating the reactive oxygen species (ROS)-mediated PI3K/AKT/GSK3 β signaling pathway.¹⁰ Apolipoprotein-J inhibits the ROS-CaMKII pathway, thereby reducing the cell injury of neonatal rat ventricular cells by preventing the augmentation of ROS.¹¹ The c-Jun NH2-terminal kinase (JNK) signaling pathway has a regulative effect on many physiological functions of organisms, such as inflammatory responses and ROS generation.¹² Additionally, the JNK signaling pathway plays a vital role in lung inflammation and injury induced by lipopolysaccharide (LPS).¹³ A study by Cheng, et al.¹⁴ indicated that mung bean polyphenol extract attenuated oxidative damage and improved the integrity of heart tissue induced by aluminum by inhibiting JNK phosphorylation. Polyphenols protect kidney mesangial cells from lead-induced renal dysfunction and intoxication both in vivo and in vitro, by inhibiting the ROS-mediated JNK-MAPK pathway.¹² Liu, et al.¹⁵ demonstrated that SH inhibits the LPS-induced mastitis in mice via the NF- κ B signaling pathway. However, the role of SH in VILI remains insufficiently studied. In this study, we detected the protective effect and mechanisms of SH on VILI, and further investigated whether the mechanism is related to the ROS-mediated JNK pathway.

MATERIALS AND METHODS

Animals and the VILI model

Male nude mice (BalbC nu/nu, 4–5 weeks old, Nanjing Biomedical Research Institute of Nanjing University, China) were anesthetized by intraperitoneal injection with 2% sodium pentobarbital (50 mg/kg), and tracheostomy was performed. The 20-gauge sterilized plastic catheter (Cusabio, Wuhan, China) was intubated into the trachea, which was connected to an animal ventilator (Kent Scientific Corporation, Torrington, CT, USA) with pre-set parameters. The parameters of the animal ventilator were as follows: tidal volume of 40 mL/kg, respiratory rate of 70 breaths/min, fraction of inspired oxygen of 21%, and inspiration:expiration ratio of 1:2. During the experiment, anesthesia was added regularly, and MV was continued for 4 hours.

Grouping and administration

The mice were divided into five groups: 1) Sham group: mice underwent intubation but spontaneously breathed. The mice were administered normal saline by gavage for 28 days; 2) VILI group: mice underwent intubation and mechanically ventilated for 4 hours. The mice were administered normal saline by gavage for 28 days; 3) SH group: mice underwent intubation but spontaneously breathed. The mice were administered 40 mg/kg SH by gavage for 28 days; 4) VILI+SH (10, 20, and 40 mg/kg) groups: VILI mice were administered 10, 20, or 40 mg/kg SH by gavage for 28 days; and 5) VILI+SH+Anisomycin (Anis) group: VILI mice were administered 40 mg/kg SH

by gavage every day and given 0.1 mg/kg Anis by intraperitoneal injection every other day for 28 days.

Collection of lung tissues

On the 29th day, all mice were euthanized with a fatal dose of sodium pentobarbital. The right lung was used for hematoxylin-eosin (HE) staining, terminal-deoxynucleotidyl transferase/(TdT)-mediated nick end labelling (TUNEL) assay, wet/dry (W/D) ratio calculation, determining ROS and malonaldehyde (MDA) levels, and detection of inflammatory factors. The left lung was used for collecting the bronchoalveolar lavage fluid (BALF).

HE staining

The upper right lung lobe was fixed in 10% formaldehyde and then embedded in paraffin. Paraffin-embedded lung tissues were divided into 4- μ m sections. The sections were deparaffinized with xylene and stained with HE. The histological changes in lung tissues were observed under a light microscope at 200 \times magnification.

TUNEL assay

The cell apoptosis in lung tissues was determined using a TUNEL kit (Roche, Basel, Switzerland). The sections of lung tissues were incubated in a humidified chamber with the TUNEL reaction mixture. Thereafter, the color was developed by using 3,3-diaminobenzidine (Sigma Aldrich, St. Louis, MO, USA). Five regions were randomly selected to count the TUNEL-positive cells, and the proportion of TUNEL-positive cells was calculated.

W/D ratio of lung tissues

The right lung middle lobe was weighed after the surface liquid was removed using absorbent paper, and the value was taken as the wet weight (W). The lobe was then placed in an oven until the weight was consistent, and the value was taken as the dry weight (D). The W/D ratio was calculated as a measure of the severity of pulmonary oedema.

BALF and cell count

BALF was obtained by three intratracheal injections of PBS. The BALF was centrifuged at 400 \times g at 4 $^{\circ}$ C for 10 min, and the total cell numbers were counted by a hemocytometer. Smears of BALF cells were stained with Giemsa to determine the neutrophil and macrophage counts.

Cell stretch experiments and SH treatment

The murine respiratory epithelial cells, MLE-15 cells, were purchased from Shanghai Zishi Biotechnology Co., Ltd. (Shanghai, China), and maintained in DMEM (Sigma Aldrich) supplemented with FBS (Invitrogen, Carlsbad, CA, USA) at 37 $^{\circ}$ C in a humidified atmosphere of 5% CO $_2$. The cell stretch (CS) experiments were performed by using FX-5000TTM Flexcell Tension

Plus (Flexcell International Corp., Burlington, VT, USA). The cells were seeded into 6-well collagen I-coated BioFlex™ culture plates and exposed to 18% CS for 4 h to mimic MV-induced cell injury. Cells cultured in the same plates but left non-stretched were used as the control group.

MLE-15 cells were divided into the following groups: 1) Control group, MLE-15 cells without treatment; 2) CS group, MLE-15 cells were exposed to 18% CS for 4 h; 3) CS+SH (25, 50, and 100 mM) groups, MLE-15 cells were pretreated with SH (25, 50, or 100 mM) prior to CS treatment; 4) CS+SH+Anis group, MLE-15 cells were pretreated with SH (100 mM) and Anis (5 μM) prior to CS treatment; and 5) CS+SH+SP600125 group, MLE-15 cells were pretreated with SH (100 mM) and SP600125 (10 μM, Calbiochem, San Diego, CA, USA) prior to CS treatment.

Flow cytometry-based analysis of apoptosis

The apoptosis of MLE-15 cells after CS experiments was measured using an annexin V/PI kit (Thermo Fisher, Waltham, MA, USA). Briefly, cells were collected and washed with PBS followed by resuspending in binding buffer containing annexin V-FITC and propidium iodide (PI). The mixture was incubated in the dark at room temperature for 30 min, and the apoptosis of cells was detected using a flow cytometer (BD, Franklin Lakes, NJ, USA).

Inflammatory factors in lung tissues and cells

The lower right lung lobe tissues (or cells) were homogenized in PBS containing 0.05% Tween 20. Thereafter, the levels of TNF- α , IL-1 β , and IL-6 were measured by using enzyme-linked immuno sorbent assay (ELISA) kits (Thermo Fisher Scientific). All operations were performed in strict accordance with the manufacturer's instructions.

ROS and MDA levels in lung tissues and cells

The ROS level in lung tissues was measured using the OxiSelect™ In Vitro ROS/RNS Assay kit (ABIN2345012, Cell Biolabs, Inc., San Diego, CA, USA). Briefly, lung tissues were homogenized in PBS, and the homogenate was centrifuged at 10000×g for 5 min. The sample was plated in a 96-well plate, and 50 μL of catalyst was added to each well, followed by incubation at room temperature for 5 min. Thereafter, 100 μL of DCFH solutions was added, followed by incubation at room temperature in the dark for 20 min. Fluorescence was read with a Multimode Reader (Thermo Fisher Scientific, Waltham, MA, USA) at 488 nm excitation/530 nm emission.

MLE-15 cells were seeded into 12-well plates (1×10^5 cells/well) and incubated overnight. The cells were treated with SH (100 mM) for 24 h. The intracellular ROS level was measured by using the Reactive Oxygen Species Assay Kit (Qcbio S&T, Shanghai, China). The DCFH-DA diluent was added to the cells followed by 30 min incubation at 37°C, and the cells were analyzed by flow cytometry.

The MDA levels were measured by using the corresponding kits (Beyotime, Shanghai, China) according to the manufacturer's instructions.

Western blot

Lung tissues or MLE-15 cells were lysed with RIPA containing protease inhibitors to obtain the total protein (Thermo Fisher Scientific). The protein was separated by 10% SDS-PAGE and then transferred to a PVDF membrane. The primary antibodies against JNK (1:1000, #9252; Cell Signaling Technology, Danvers, MA, USA), p-JNK (1:1000, #9255; Cell Signaling Technology), Bcl-2 (1:1000, SAB4500003; Sigma Aldrich), Bax (1:1000, B8429; Sigma Aldrich), and Bak (1:1000, SAB4502532; Sigma Aldrich) were incubated with the membrane at 4°C overnight. Thereafter, the membranes were incubated with secondary antibody (1:5000, Sigma Aldrich) at room temperature for 40 min. The bands were visualized with ECL detection reagents (GE Healthcare, Little Chalfont, Buckinghamshire, UK). GAPDH served as the internal reference, and the ratio of the gray value of target band to internal reference band was considered as the relative protein level. ImageJ software (National Institutes of Health, Bethesda, MD, USA) was used to analyze the gray value.

Ethics approval and consent

The experimental protocol of our study was performed in accordance with the Guide for the Care and Use of Laboratory Animals and approved by the Affiliated Huaian No.1 People's Hospital of Nanjing Medical University (IACUC no.: HAN 120180302).

Statistical analysis

Data are expressed as mean \pm SD from three independent experiments. The differences between groups were analyzed by the SPSS 21.0 software (IBM Corp., Armonk, NY, USA) using Student's t-test or one-way analysis of variance. A *p*-value <0.05 was considered statistically significant.

RESULTS

SH relieves VILI in mice

In order to measure the effect of SH on VILI in mice, the pathological changes, apoptosis, and pulmonary oedema of lung tissues were detected after SH gavage of VILI mice. Compared to the Sham group, VILI modelling damaged the structural integrity of lung tissues (Fig. 1A), increased TUNEL-positive cells, accelerated apoptosis (Fig. 1B), and caused pulmonary oedema (Fig. 1C). SH gavage reduced lung injury, apoptosis in lung tissues, and the W/D ratio in VILI mice (Fig. 1B and C), and the relieving effect of SH on lung injury was gradually enhanced with an increased dose. Considering the best protection effect on lung injury in VILI mice, 40 mg/kg was selected

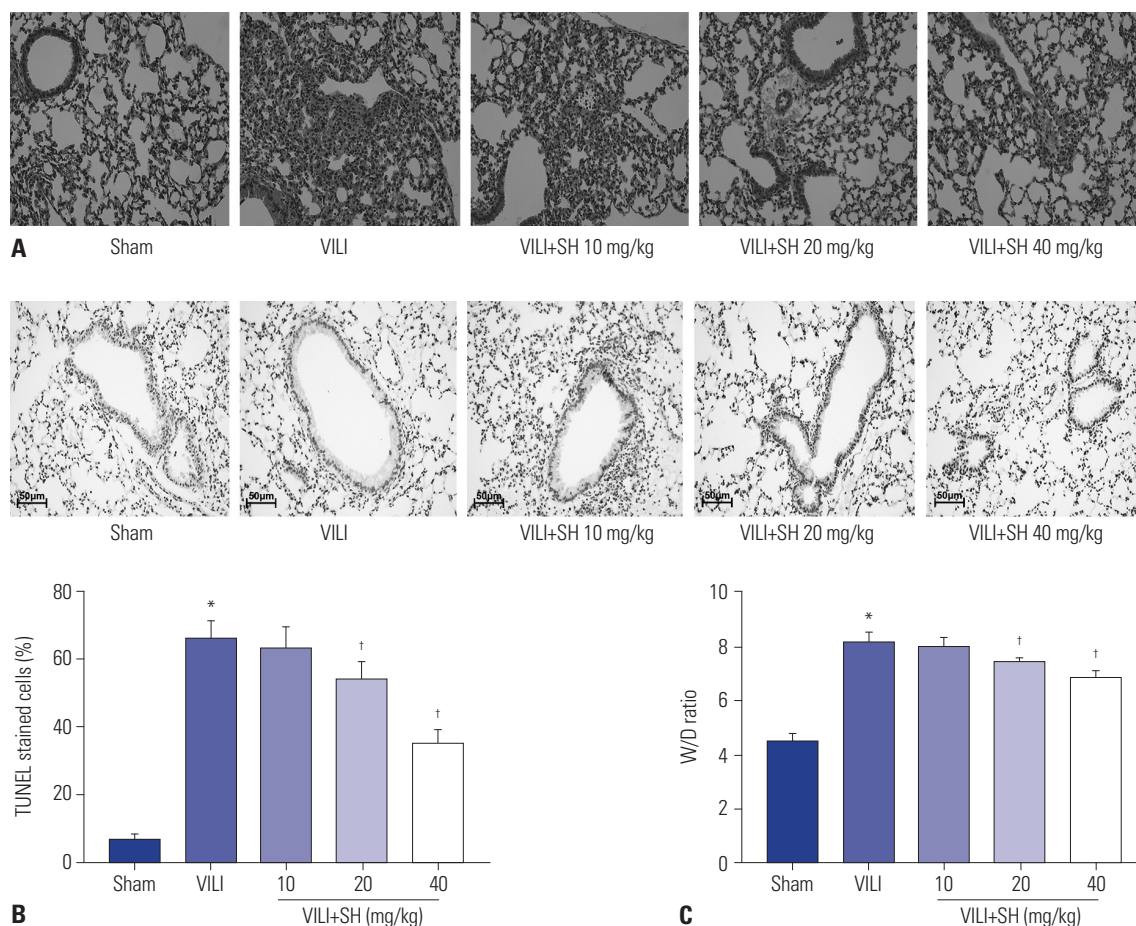


Fig. 1. SH relieves VILI in mice. (A) The pathological changes of lung tissues measured by HE staining ($\times 200$). (B) The apoptosis of lung tissues measured by TUNEL staining (scale bars, 50 μm). (C) The W/D ratio of lung tissues. * $p < 0.05$ vs. Sham group, [†] $p < 0.05$ vs. VILI group. SH, sodium houttuynonate; VILI, ventral-tor-induced lung injury; W/D, wet-to-dry.

among the three doses of SH for the subsequent experiments.

SH reduces ROS level and inhibits JNK pathway

In this study, we found that the protein expression of p-JNK/JNK in VILI group was significantly higher than that in Sham group, while SH gavage (40 mg/kg) sharply decreased the p-JNK/JNK expression in VILI group ($p < 0.05$) (Fig. 2A). To confirm the effect of JNK pathway on VILI, the JNK activator Anis was intraperitoneally administered to VILI mice after the SH gavage. The data showed that the protein expression of p-JNK/JNK was significantly increased in VILI+SH+Anis group compared to the VILI+SH group ($p < 0.05$). We then measured the apoptosis and W/D ratio of lung tissues. The results suggested that SH gavage remarkably decreased the TUNEL-stained cell levels and W/D ratio, while intraperitoneal injection of Anis significantly increased the apoptosis cells and W/D ratio of lung tissues ($p < 0.05$) (Fig. 2B and C). Western blot data indicated that the protein expression of Bcl-2 was significantly decreased, and those of Bax and Bak were significantly increased in VILI group compared to Sham group ($p < 0.05$) (Fig. 2A). SH gavage markedly enhanced the protein expression of Bcl-2 and re-

duced the protein expression of Bax and Bak ($p < 0.05$). After intraperitoneal injection of Anis, the protein expression of Bcl-2 was remarkably reduced, while those of Bax and Bak were markedly increased ($p < 0.05$). Additionally, we detected the effect of SH on ROS and MDA in VILI mice. The levels of ROS and MDA in VILI group were significantly higher than those in Sham group ($p < 0.05$) (Fig. 2D and E). The increased levels of ROS and MDA were remarkably decreased by SH gavage ($p < 0.05$). However, the JNK activator Anis significantly increased the levels of ROS and MDA reduced by SH gavage ($p < 0.05$).

JNK activator eliminates the inhibitory effects of SH on inflammation in VILI mice

The inflammation levels in lung tissues were measured by ELISA kits. The data showed that VILI modelling markedly increased the levels of TNF- α , IL-1 β , and IL-6 in lung tissues ($p < 0.05$) (Fig. 3A). The total numbers of cells, neutrophils, and macrophages in BALF in VILI group were increased markedly compared to those in Sham group ($p < 0.05$) (Fig. 3B). Compared to VILI group, SH gavage (20 mg/kg) sharply decreased the levels of TNF- α , IL-1 β , and IL-6 in lung tissues, and reduced the

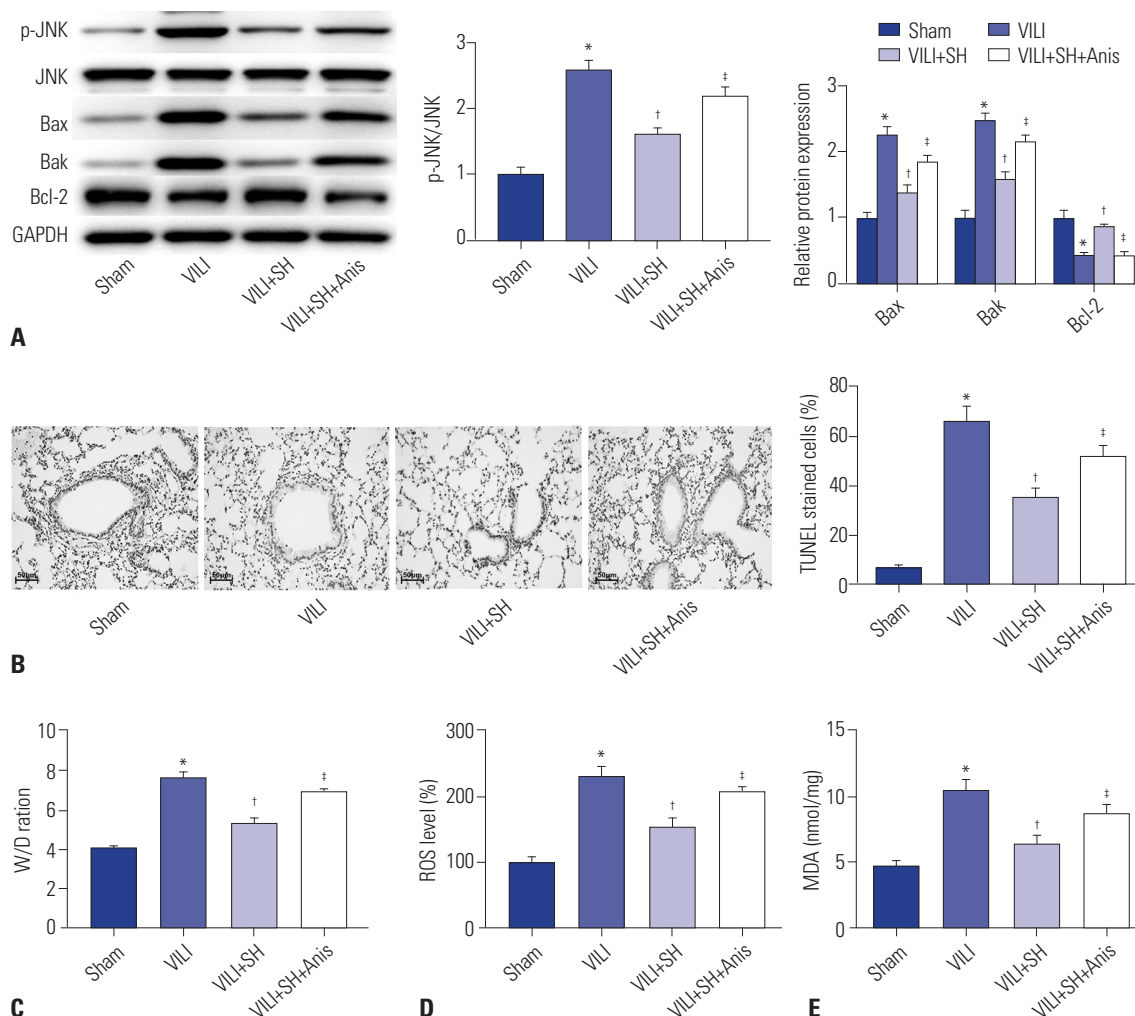


Fig. 2. SH inhibits the JNK pathway and reduces the levels of ROS inflammation. (A) The protein expression of p-JNK/JNK, Bcl-2, Bax, and Bak was detected by Western blot. (B) The apoptosis of lung tissues measured by TUNEL staining (scale bars, 50 μ m). (C) The W/D ratio of lung tissues. (D and E) The levels of ROS and MDA in lung tissues. * $p < 0.05$ vs. Sham group, † $p < 0.05$ vs. VILI group, ‡ $p < 0.05$ vs. VILI+SH group. The gavage dose of SH was 40 mg/kg. SH, sodium houthuyfonate; ROS, reactive oxygen species; VILI, ventralitor-induced lung injury; W/D, wet-to-dry; MDA, malonaldehyde.

total numbers of cells, neutrophils, and macrophages in BALF ($p < 0.05$). However, the JNK activator Anis eliminated the inhibitory effect of SH on inflammation and the total cell number in BALF ($p < 0.05$).

SH decreases cell apoptosis induced by CS experiment and inhibits JNK pathway

To further confirm the effect of SH on VILI, the CS experiment was performed using the murine respiratory epithelial cells, MLE-15, to simulate the stretching of MV. The data showed that CS treatment significantly increased the apoptosis rate of MLE-15 cells compared to the Control group ($p < 0.05$) (Fig. 4A). Compared to CS group, SH treatment decreased the apoptosis of MLE-15 cells in a dose-dependent manner ($p < 0.05$).

We detected the protein expression of p-JNK/JNK, Bcl-2, Bax, and Bak in MLE-15 cells by Western blot. The results indicated that CS treatment increased the protein expression of p-JNK/JNK, Bax, and Bak, and decreased the Bcl-2 protein ex-

pression in MLE-15 cells compared to Control group ($p < 0.05$) (Fig. 4B). The protein expression of p-JNK/JNK, Bax, and Bak in CS+SH (100 mM) group was considerably lower, while that of Bcl-2 was higher compared to CS group ($p < 0.05$) (Fig. 4B). Compared to CS+SH group, the JNK activator Anis significantly down-regulated the Bcl-2 protein expression and up-regulated the protein expression of p-JNK/JNK, Bax, and Bak in MLE-2 cells ($p < 0.05$). In addition, Anis treatment reversed the inhibitory effect of SH on apoptosis of MLE-15 cells, and accelerated apoptosis of MLE-15 cells ($p < 0.05$) (Fig. 4C).

JNK activator eliminates the inhibitory effects of SH on ROS and inflammation in CS-induced MLE-15 cells

We measured the levels of ROS and MDA in MLE-15 cells after the CS experiment. The data showed that CS treatment significantly enhanced the levels of ROS and MDA ($p < 0.05$) (Fig. 5A and B). Compared with CS group, SH treatment (100 mM) sharply decreased the levels of ROS and MDA in MLE-

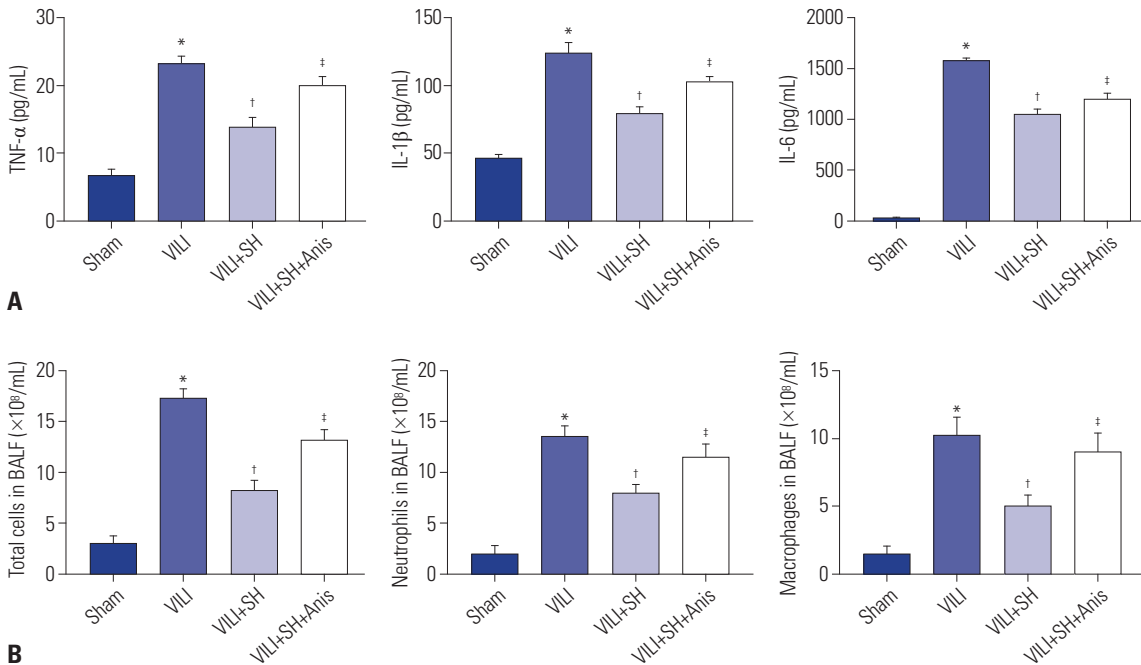


Fig. 3. SH reduces inflammation of VILI mice. (A) The levels of TNF-α, IL-1β, and IL-6 in lung tissues measured by ELISA kits. (B) Total cell, neutrophil, and macrophage counts in BALF. **p*<0.05 vs. Sham group, †*p*<0.05 vs. VILI group, ‡*p*<0.05 vs. VILI+SH group. The gavage dose of SH was 40 mg/kg. SH, sodium houttuyfonate; VILI, ventralitor-induced lung injury; W/D, wet-to-dry; BALF, bronchoalveolar lavage fluid.

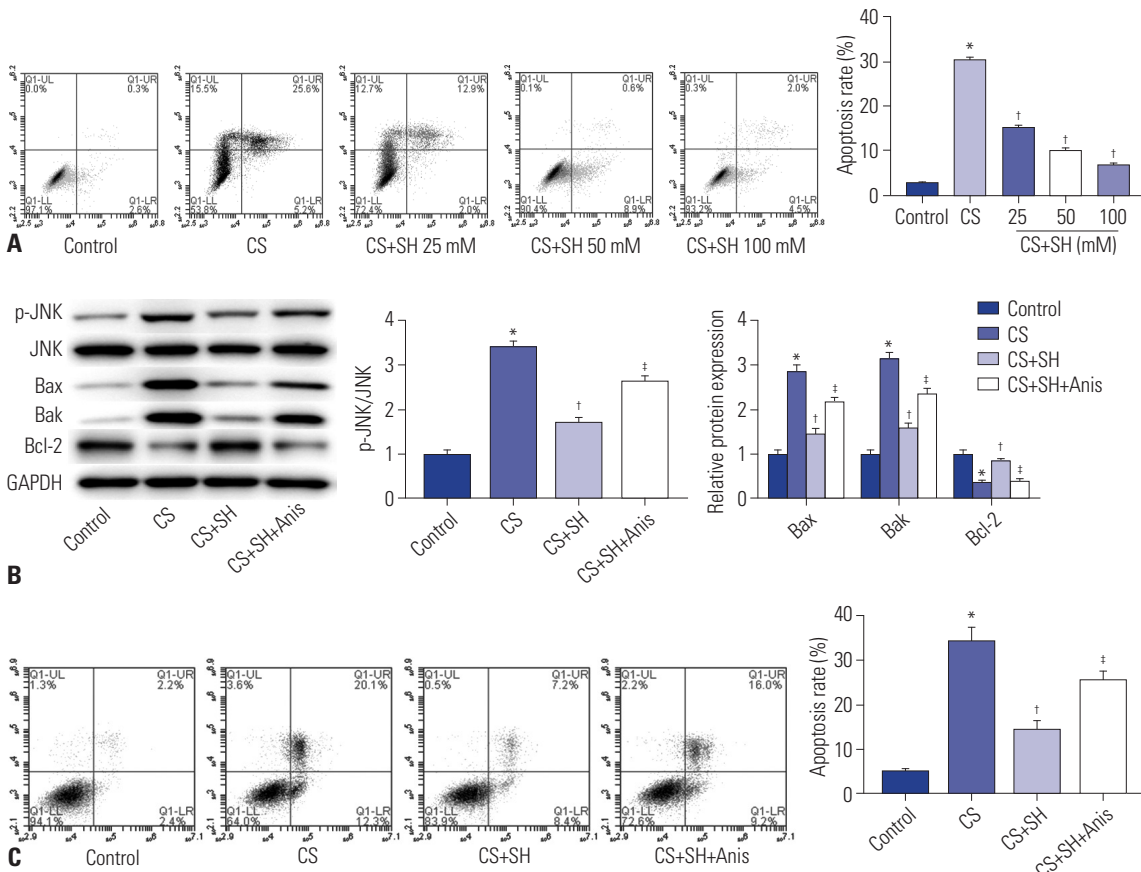


Fig. 4. SH decreases cell apoptosis induced by CS experiment and inhibits JNK pathway. (A and C) The apoptosis of MLE-15 cells was detected by flow cytometry. (B) The protein expression of p-JNK/JNK, Bcl-2, Bax, and Bak was measured by Western blot. **p*<0.05 vs. Control group, †*p*<0.05 vs. CS group, ‡*p*<0.05 vs. CS+SH group. SH, sodium houttuyfonate; CS, cell stretch.

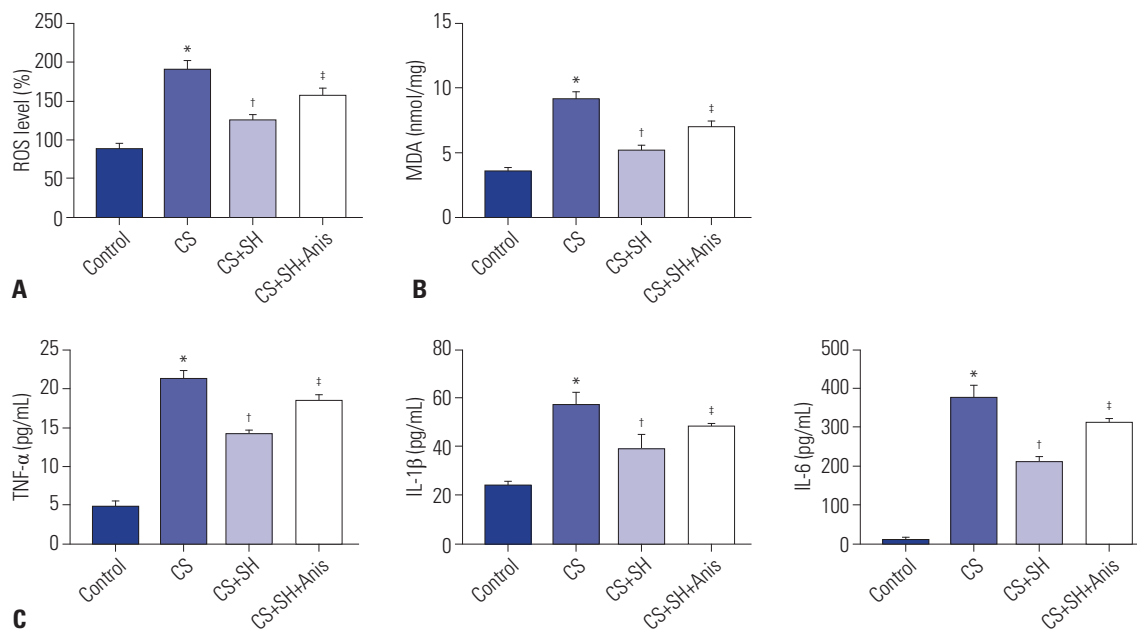


Fig. 5. JNK activator eliminates the inhibitory effects of SH on ROS and inflammation in CS-induced MLE-15 cells. (A and B) The levels of ROS and MDA in MLE-15 cells. (C) The levels of TNF- α , IL-1 β , and IL-6 in MLE-15 cells were measured by ELISA kits. * $p < 0.05$ vs. Control group, † $p < 0.05$ vs. CS group, ‡ $p < 0.05$ vs. CS+SH group. The dose of SH was 100 mM. SH, sodium houthuyfonate; CS, cell stretch; ROS, reactive oxygen species; MDA, malonaldehyde.

15 cells ($p < 0.05$). However, activation of JNK pathway increased the levels of ROS and MDA ($p < 0.05$). The levels of inflammatory factors (TNF- α , IL-1 β , and IL-6) in MLE-15 cells were measured by ELISA. The results indicated that CS treatment markedly increased the levels of TNF- α , IL-1 β , and IL-6 in MLE-15 cells ($p < 0.05$) (Fig. 5C). Compared to CS group, the inflammation levels in CS+SH group were significantly decreased ($p < 0.05$). Besides, the inflammation levels in CS+SH+Anis group were significantly enhanced compared to CS+SH group ($p < 0.05$).

JNK inhibitor strengthens the inhibitory effects of SH on ROS and inflammation in CS-induced MLE-15 cells

To further confirm that the JNK pathway is involved in ROS and inflammation in CS-induced cells, we measured the levels of ROS and MDA of CS-treated MLE-15 cells after the treatment of JNK inhibitor SP600125. As shown in Fig. 6A, the protein expression of p-JNK/JNK in CS+SH+SP600125 group was markedly decreased compared to CS+SH group ($p < 0.05$). The data displayed in Fig. 6B and C showed that JNK inhibitor SP600125 significantly reduced the levels of ROS and MDA in CS+SH group ($p < 0.05$). The ELISA results indicated that the levels of inflammatory factors (TNF- α , IL-1 β , and IL-6) in CS+SH+SP600125 group were markedly lower than those in CS+SH group ($p < 0.05$) (Fig. 6D).

DISCUSSION

VILI is a serious complication of MV that increases morbidity

rates and mortality of patients receiving ventilator treatment.¹ VILI severely disrupts the integrity of lung function, leading to increased lung permeability and inflammatory factor levels.¹⁶ In our study, SH alleviated lung injury in VILI mice by reducing the levels of ROS and inflammation, and the protective effect of SH on VILI was achieved by inhibiting ROS-mediated JNK pathway.

SH can be used for the treatment of many diseases, including myocardial infarction, mastitis, and COPD.^{9,15,17,18} The findings of Zheng, et al.¹⁷ showed that long-term SH treatment improves left ventricular function and reduces histopathological changes caused by myocardial infarction. Similar results were obtained in our research. In our study, SH gavage substantially relieved lung injury and inhibited apoptosis in VILI mice. SH treatment inhibited the apoptosis of MLE-15 cells induced by CS experiments. Besides, the high expression levels of Bax and Bak induced by VILI modelling, and CS experiment was significantly down-regulated by SH treatment. These data indicated that SH gavage may relieve lung injury in VILI mice by reducing the apoptosis in lung tissues.

The infiltration of inflammatory cells and an increase in TNF- α , IL-1 β , IL-6, and other inflammatory factor levels due to mechanical forces during MV are the main characteristics of VILI.¹⁹⁻²¹ Boehm, et al.²² found that the protein expression of TNF- α , IL-1 β , and IL-6 in high tidal volume ventilation pre-treated mice was significantly increased. A study by Ye, et al.²³ revealed that mice subjected to high tidal ventilation for 4 h showed severe pulmonary oedema and inflammation compared to mice with spontaneous breathing. Suppressing the levels of inflammation could alleviate lung injury of VILI. Zhu,

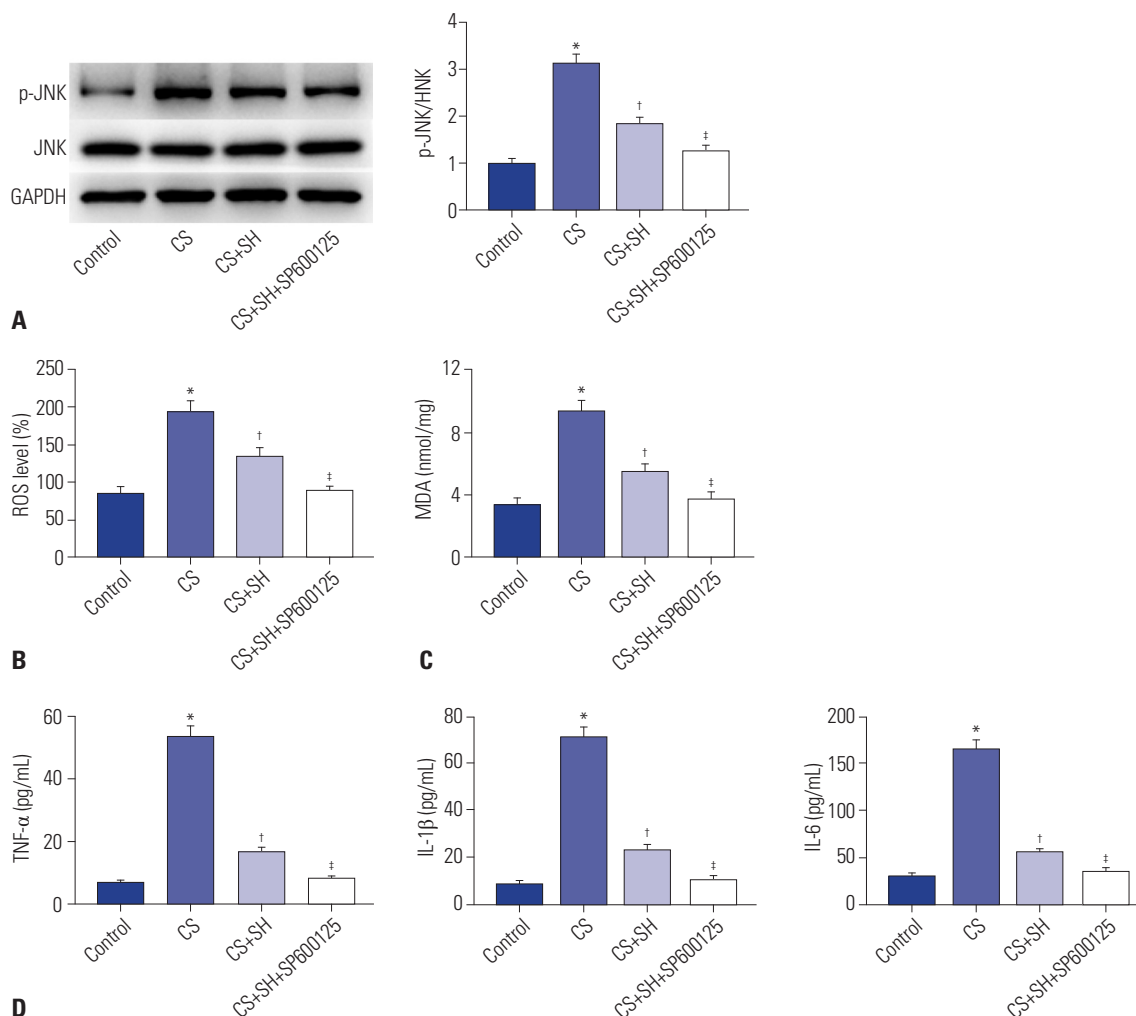


Fig. 6. JNK inhibitor strengthens the inhibitory effects of SH on ROS and inflammation in CS-induced MLE-15 cells. (A) The protein expression of p-JNK/JNK was measured by Western blot. (B and C) The levels of ROS and MDA in MLE-15 cells. (D) The levels of TNF- α , IL-1 β , and IL-6 in MLE-15 cells were measured by ELISA kits. * $p < 0.05$ vs. Control group, † $p < 0.05$ vs. CS group, ‡ $p < 0.05$ vs. CS+SH group. The dose of SH was 100 mM. SH, sodium houttuynonate; CS, cell stretch; ROS, reactive oxygen species; MDA, malonaldehyde.

et al.²⁴ demonstrated that SH decreases the protein expression of TNF- α , IL-1 β , and IL-6 in LPS-induced bovine endometrial epithelial cell. In addition, the total cells, neutrophil, and macrophage counts in BALF are increased in VILI.^{25,26} Ju, et al.²⁷ found that the neutrophil count in BALF of VILI rats decreased significantly after VE treatment. Lin, et al.²⁸ showed that the total cells, neutrophil, and macrophage counts in BALF of VILI rats with ARDS were significantly higher than those in Sham rats. In our study, the levels of inflammatory factors (TNF- α , IL-1 β , and IL-6) were significantly higher in VILI models and CS-treated cells. SH treatment significantly decreased inflammatory factor levels. In addition, the total cells, neutrophil, and macrophage counts in BALF were markedly reduced by SH gavage. The W/D ratio of VILI mice was also reduced by SH gavage. All of these results indicated that SH may reduce lung injury in VILI mice by decreasing the inflammatory factor levels.

ROS are generally recognized as one of the secondary mes-

engers that amplify inflammation by activating downstream signals.²⁹ ROS may facilitate various signaling processes, including autophagy, immune responses, and inflammation.^{30,31} The inhibition of ROS production may alleviate LPS-induced acute lung injury.³² Pretreatment of mouse epithelial cells with ROS scavengers significantly reduces LPS-induced apoptosis.³³ The ROS-mediated JNK pathway is widely involved in the development of many diseases, including cardiac injury, intervertebral disc degeneration, and myocardial ischemia-reperfusion injury.^{18,34} Pretreatment with NAC (a ROS scavenger) significantly reduces NMDA-induced JNK phosphorylation, indicating the involvement of ROS in JNK pathway.³⁵ Chen, et al.³⁶ found that inhibiting JNK phosphorylation reduced ROS production in acute stress-induced kidney injury. Silencing of JNK inhibits the apoptosis of Leydig TM3 cells induced by cadmium.³⁷ The activation of JNK pathway promotes the apoptosis of myocardial cells in rats after myocardial ischemia and reperfusion.³⁸ In this study, we found that the levels of p-JNK/JNK,

ROS, and MDA were increased in both VILI mice and CS-treated MLE-15 cells. SH treatment could inhibit the JNK pathway, decrease the levels of ROS and MDA, and reduce the apoptosis in lung tissues and MLE-15 cells. JNK pathway activator Anis could significantly aggravate lung injury in VILI mice. The results of the in vitro experiment showed that the activation of JNK pathway increased ROS levels and cell apoptosis. The JNK inhibitor SP600125 reduced p-JNK/JNK and ROS levels in CS-treated cells. These results suggested that the activation of JNK pathway weakened the protective effect of SH, whereas the inhibition of JNK pathway strengthened the protective effect of SH on VILI.

In conclusion, VILI modeling remarkably increased the levels of inflammatory factors and ROS, activated the ROS-mediated JNK pathway, and induced apoptosis in lung tissues. SH gavage could inhibit the production of ROS and reduce the inflammatory factor levels and JNK phosphorylation, thereby relieving lung injury. However, JNK activator Anis eliminated the protective effect of SH on VILI. The findings of our study offer potential therapeutic ideas for the treatment of VILI. Nevertheless, further research is still required, as the mechanism of VILI is complex.

AUTHOR CONTRIBUTIONS

Conceptualization: Jinyu Li. **Data curation:** Gang Tang. **Formal analysis:** Gang Tang. **Funding acquisition:** Yi Liu and Jinyu Li. **Investigation:** Jinyu Li. **Methodology:** Gang Tang. **Project administration:** Jinyu Li. **Resources:** Jinyu Li. **Software:** Yi Liu and Jinyu Li. **Supervision:** Jinyu Li. **Validation:** Yi Liu. **Visualization:** Yi Liu and Jinyu Li. **Writing—original draft:** Yi Liu. **Writing—review & editing:** all authors. **Approval of final manuscript:** all authors.

ORCID iDs

Yi Liu <https://orcid.org/0000-0002-6772-6813>
 Gang Tang <https://orcid.org/0000-0002-2147-4446>
 Jinyu Li <https://orcid.org/0000-0002-3489-065X>

REFERENCES

- Gattinoni L, Tonetti T, Cressoni M, Cadringer P, Herrmann P, Moerer O, et al. Ventilator-related causes of lung injury: the mechanical power. *Intensive Care Med* 2016;42:1567-75.
- Slutsky AS, Ranieri VM. Ventilator-induced lung injury. *N Engl J Med* 2013;369:2126-36.
- Kuchnicka K, Maciejewski D. Ventilator-associated lung injury. *Anaesthesiol Intensive Ther* 2013;45:164-70.
- Fan E, Brodie D, Slutsky AS. Acute respiratory distress syndrome: advances in diagnosis and treatment. *JAMA* 2018;319:698-710.
- Fan E, Del Sorbo L, Goligher EC, Hodgson CL, Munshi L, Walkey AJ, et al. An Official American Thoracic Society/European Society of Intensive Care Medicine/Society of Critical Care Medicine clinical practice guideline: mechanical ventilation in adult patients with acute respiratory distress syndrome. *Am J Respir Crit Care Med* 2017;195:1253-63.
- Shao J, Cheng H, Wang C, Wang Y. A phytoanticipin derivative, sodium houttuynonate, induces in vitro synergistic effects with levofloxacin against biofilm formation by *Pseudomonas aeruginosa*. *Molecules* 2012;17:11242-54.
- Wang W, Hu X, Shen P, Zhang N, Fu Y. Sodium houttuynonate inhibits LPS-induced inflammatory response via suppressing TLR4/NF- κ B signaling pathway in bovine mammary epithelial cells. *Microb Pathog* 2017;107:12-6.
- Tang W, Xia YZ, Liu JX, Liu L, Yan Y. Effects of sodium houttuynonate on spinal cord injured neurons in rats. *J Shanghai Jiaotong Univ (Med Sci)* 2017;37:1594-600.
- Wu Z, Tan B, Zhang H, Guo Y, Tu Y, Qiu F, et al. Effects of sodium houttuynonate on pulmonary inflammation in COPD model rats. *Inflammation* 2017;40:2109-17.
- Deng S, Dai G, Chen S, Nie Z, Zhou J, Fang H, et al. Dexamethasone induces osteoblast apoptosis through ROS-PI3K/AKT/GSK3 β signaling pathway. *Biomed Pharmacother* 2019;110:602-8.
- Ma Y, Gong Z, Nan K, Qi S, Chen Y, Ding C, et al. Apolipoprotein-J blocks increased cell injury elicited by ox-LDL via inhibiting ROS-CaMKII pathway. *Lipids Health Dis* 2019;18:117.
- Wang H, Li D, Hu Z, Zhao S, Zheng Z, Li W. Protective effects of green tea polyphenol against renal injury through ROS-mediated JNK-MAPK pathway in lead exposed rats. *Mol Cells* 2016;39:508-13.
- Ying H, Kang Y, Zhang H, Zhao D, Xia J, Lu Z, et al. MiR-127 modulates macrophage polarization and promotes lung inflammation and injury by activating the JNK pathway. *J Immunol* 2015;194:1239-51.
- Cheng D, Wang R, Wang C, Hou L. Mung bean (*Phaseolus radiatus* L.) polyphenol extract attenuates aluminum-induced cardiotoxicity through an ROS-triggered Ca²⁺/JNK/NF- κ B signaling pathway in rats. *Food Funct* 2017;8:851-9.
- Liu P, Yang C, Lin S, Zhao G, Zhang T, Guo S, et al. Sodium houttuynonate inhibits LPS-induced mastitis in mice via the NF- κ B signaling pathway. *Mol Med Rep* 2019;19:2279-86.
- Wagner J, Strosing KM, Spassov SG, Lin Z, Engelstaedter H, Tacke S, et al. Sevoflurane posttreatment prevents oxidative and inflammatory injury in ventilator-induced lung injury. *PLoS One* 2018;13:e0192896.
- Zheng C, Lin JF, Lin ZH, Lin WQ, Thapa S, Lin YZ, et al. Sodium houttuynonate alleviates post-infarct remodeling in rats via AMP-activated protein kinase pathway. *Front Pharmacol* 2018;9:1092.
- Ge J, Cheng X, Yuan C, Qian J, Wu C, Cao C, et al. Syndecan-4 is a novel therapeutic target for intervertebral disc degeneration via suppressing JNK/p53 pathway. *Int J Biol Sci* 2020;16:766-76.
- Sutherasan Y, Vargas M, Pelosi P. Protective mechanical ventilation in the non-injured lung: review and meta-analysis. *Crit Care* 2014;18:211.
- Delong P, Murray JA, Cook CK. Mechanical ventilation in the management of acute respiratory distress syndrome. *Semin Dial* 2006;19:517-24.
- Samary CS, Silva PL, Gama de Abreu M, Pelosi P, Rocco PR. Ventilator-induced lung injury: power to the mechanical power. *Anesthesiology* 2016;125:1070-1.
- Boehm O, Rohner M, Ehrentraut H, Guenther U, Meyer R, Knuefermann P, et al. Low-tidal-volume prevent ventilation induced inflammation in a mouse model of sepsis. *Life Sci* 2020;240:117081.
- Ye L, Zeng Q, Dai H, Zhang W, Wang X, Ma R, et al. Endoplasmic reticulum stress is involved in ventilator-induced lung injury in mice via the IRE1 α -TRAF2-NF- κ B pathway. *Int Immunopharmacol* 2020;78:106069.
- Zhu Q, Xu X, Liu X, Lin J, Kan Y, Zhong Y, et al. Sodium houttuynonate inhibits inflammation by blocking the MAPKs/NF- κ B signaling pathways in bovine endometrial epithelial cells. *Res Vet Sci* 2015;100:245-51.

25. Zheng J, Huang Y, Islam D, Wen XY, Wu S, Streutker C, et al. Dual effects of human neutrophil peptides in a mouse model of pneumonia and ventilator-induced lung injury. *Respir Res* 2018;19:190.
26. Zhu H, He J, Liu J, Zhang X, Yang F, Liu P, et al. Alpha 1-antitrypsin ameliorates ventilator-induced lung injury in rats by inhibiting inflammatory responses and apoptosis. *Exp Biol Med (Maywood)* 2018;243:87-95.
27. Ju YN, Geng YJ, Wang XT, Gong J, Zhu J, Gao W. Endothelial progenitor cells attenuate ventilator-induced lung injury with large-volume ventilation. *Cell Transplant* 2019;28:1674-85.
28. Lin X, Ju YN, Gao W, Li DM, Guo CC. Desflurane attenuates ventilator-induced lung injury in rats with acute respiratory distress syndrome. *Biomed Res Int* 2018;2018:7507314.
29. Yang CS, Kim JJ, Lee SJ, Hwang JH, Lee CH, Lee MS, et al. TLR3-triggered reactive oxygen species contribute to inflammatory responses by activating signal transducer and activator of transcription-1. *J Immunol* 2013;190:6368-77.
30. Bae YS, Oh H, Rhee SG, Yoo YD. Regulation of reactive oxygen species generation in cell signaling. *Mol Cells* 2011;32:491-509.
31. Forman HJ, Torres M. Reactive oxygen species and cell signaling: respiratory burst in macrophage signaling. *Am J Respir Crit Care Med* 2002;166(12 Pt 2):S4-8.
32. Liu S, Yue Y, Pan P, Zhang L, Su X, Li H, et al. IRF-1 intervention in the classical ROS-dependent release of NETs during LPS-induced acute lung injury in mice. *Inflammation* 2019;42:387-403.
33. Yanling Q, Xiaoning C, Fei B, Liyun F, Huizhong H, Daqing S. Inhibition of NLRP9b attenuates acute lung injury through suppressing inflammation, apoptosis and oxidative stress in murine and cell models. *Biochem Biophys Res Commun* 2018;503:436-43.
34. Zhu Z, Huang Y, Lv L, Tao Y, Shao M, Zhao C, et al. Acute ethanol exposure-induced autophagy-mediated cardiac injury via activation of the ROS-JNK-Bcl-2 pathway. *J Cell Physiol* 2018;233:924-35.
35. Yang X, Zhang H, Wu J, Yin L, Yan LJ, Zhang C. Humanin attenuates NMDA-induced excitotoxicity by inhibiting ROS-dependent JNK/p38 MAPK pathway. *Int J Mol Sci* 2018;19:2982.
36. Chen Y, Feng X, Hu X, Sha J, Li B, Zhang H, et al. Dexmedetomidine ameliorates acute stress-induced kidney injury by attenuating oxidative stress and apoptosis through inhibition of the ROS/JNK signaling pathway. *Oxid Med Cell Longev* 2018;2018:4035310.
37. Ren X, Wang S, Zhang C, Hu X, Zhou L, Li Y, et al. Selenium ameliorates cadmium-induced mouse leydig TM3 cell apoptosis via inhibiting the ROS/JNK /c-jun signaling pathway. *Ecotoxicol Environ Saf* 2020;192:110266.
38. Li HW, Xiao FY. Effect of hydrogen sulfide on cardiomyocyte apoptosis in rats with myocardial ischemia-reperfusion injury via the JNK signaling pathway. *Eur Rev Med Pharmacol Sci* 2020;24:2054-61.